Comparison of Different Methods of Automated Landform Classification at the Drainage Basin Scale: Examples from the Southern Italy

Dario Gioia[1](✉), Maria Danese[1], Mario Bentivenga[2], Eva Pescatore[2], Vincenzo Siervo[2], and Salvatore Ivo Giano[2]

[1] ISPC-CNR, Tito, Potenza, Italy
dario.gioia@cnr.it
[2] Facoltà di Scienze, Università della Basilicata, Potenza, Italy

Abstract. In this work, we tested the reliability of two different methods of automated landform classification (ACL) in three geological domains of the southern Italian chain with contrasting morphological features. ACL maps deriving from the TPI-based (topographic position index) algorithm are strictly dependent to the search input parameters and they are not able to fully capture landforms of different size. Geomorphons-based classification has shown a higher potential and can represent a powerful method of ACL, although it should be improved with the introduction of additional DEM-based parameters for the extraction of landform classes.

Keywords: Geomorphometry · Automatic landform classification · Geomorphological mapping · Southern Italy · DEM analysis

1 Introduction

In the last years, several factors such as availability of high-resolution DEMs, advances in computer power and the growing ability of research group to produce GIS-aided tools have promoted the development of many procedures and algorithms of automated classification/extraction of landforms [1]. Many works demonstrated that landform maps based on unsupervised classification represent a key tool in different research fields such as geomorphology, geology, archaeology, soil science and seismology [2–7]. Automatic classification of landform (ACL) provides several advantages than the traditional methods of geomorphological analysis, such as photo-interpretation and field surveys. Firstly, the use of an appropriate algorithm of landform classification overcomes the issue of the subjective interpretation of the user and the low reproducibility of "hand-made" geomorphological maps. Moreover, the full coverage of a study area can be useful in different applications, aimed at the investigation of the relationships between landforms and other parameters [8]. Although these factors should promote a fast growth of the application of ACL methods, the maps deriving by such an approach are frequently not able to fully define the spatial pattern of landforms

O. Gervasi et al. (Eds.): ICCSA 2020, LNCS 12250, pp. 696–708, 2020.
https://doi.org/10.1007/978-3-030-58802-1_50

and are affected by high-level noise. However, a relevant limitation of the method is due to its high scale-dependence. Landforms pertained to different geological landscapes have peculiar dimensions and in a first step the ACL should include the hierarchical definition of type and size of landforms occurring at different scales [1]. Most of the ACL approaches are focused on the characterization of mesoscale landforms (size-scale of hundred meters) and are strictly dependent of the search window size. Finally, this kind of approach does not provide any information about the time and origin of the geomorphic features [2], thus implying additional steps of "experts" in map interpretation.

Due to these limitations, the time-consuming traditional approaches of landform recognition and mapping are still the preferred ones by geomorphologists whereas extensive validation studies on the ACL are lacking.

In this paper, we try to fill this gap through the comparison of ACL maps coming from two of the most promising methods of automatic/semiautomatic landform extraction. The first method is the well-known TPI-based classification [9], and the second one is the geomorphons algorithm, recently proposed by [10]. Results of the ACL obtained by the two methods have been investigated in three different landscapes of southern Italy, featured by contrasting geological and geomorphological characters (Fig. 1). A comparison between two different ACL methods was carried out in the three test areas and the robustness and reliability of the two unsupervised classification methods have been discussed.

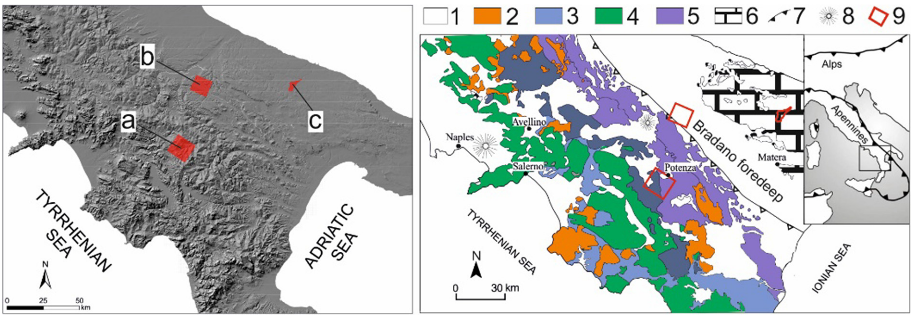

Fig. 1. (A) Geographical location (red boxes indicate study areas: a) axial zone; b) foredeep; c) foreland) and (B) geological sketch map of study areas. Legend: 1) Pliocene-Quaternary clastics and Quaternary volcanics; 2) Miocene syntectonic deposits; 3) Cretaceous to Oligocene ophiolite-bearing internal units (Ligurian units); 4) Mesozoic-Cenozoic shallow-water carbonates of the Apenninic platform; 5) Lower-middle Triassic to Miocene shallow-water and deep-sea succession of the Lagonegro unit; 6) Mesozoic-Cenozoic shallow-water carbonates of the Apulian platform; 7) Thrust front of the chain; 8) Volcanoes; 9) Study areas (Color figure online)

2 Methods

The existing methods of ACL are mainly based on the extraction of first and second orders DEM-derivative attributes (slope and curvature). Local surface shape is frequently combined to the relative slope position of the landform elements thus to group the landscape sectors with similar statistical parameters and within a selected moving windows [1, 11]. Available algorithms are strictly dependent of the moving windows size and clustering can be cell-based or object-based [12, 13].

In this work, we test the accuracy of two different procedures of ACL in three study areas where also an interpretation of the "real" landforms based on an "expert" geomorphological analysis was realized. Application of the two algorithms of automated landform classification has been carried out using high-resolution DEMs (i.e. spatial resolution of 5 m for the axial and foredeep sectors and 8 m for the foreland area) deriving from Airborne LIDAR surveys. The DEMs are freely available.

The first one is a well-known algorithm that classifies landform units through a combination of TPI value and slope thresholds. TPI-based slope classification has been performed using an ArcGIS tool developed by Jenness Enterprises [9]. The algorithm evaluates the elevation difference between a cell and the average elevation around it within a predetermined radius. Positive TPI values indicate that the pixel has an elevation value higher than the average ones of the neighborhood searching window, whereas negative values are representative of a pixel with a lower elevation than the average of the search radius. TPI is strongly influenced by the search radius dimension: in particular, a large search radius highlights major landscape units, whereas the detection of minor landforms should be performed by using a small radius [4, 6, 14]. For this reason, in the Landform Classification Tool two search radii are inserted, a smaller and a larger neighborhood, in order to try to capture different sizes or landforms. After the calculation of the TPI index, a slope position index (i.e. SPI) classification was produced, where ten discrete classes (landforms) are obtained by combining the degree to which the TPI is lower or higher than the average and some slope classes set by default in the tool.

The second method used to realize a landform map and named as geomorphon, was proposed by [10] and implemented in a Grass GIS tool. It differs from the other existing algorithms of ACL because it does not use classic map algebra methods to calculate elevation differences inside the neighborhood. Conversely, it uses a computer vision approach, a pattern-based classification that self-adapts to the local topography. This technique utilizes the line-of-sight principle to evaluate a D quantity in each surrounding; more specifically, such an approach takes in count not only the elevation differences but also the zenith and nadir angles in the profiles and the lookup distance and should ensure identification of a landform at their most appropriate spatial scale [10]. Landform classification is derived from the extraction of Local Ternary Patterns (LTP). LTP are the basic micro-structure that constitute each existing type of landform and are named geomorphons; through the combination of geomorphon, landforms are extracted, in particular the first ten classes given back by the algorithm constitute the most frequent existing landform elements [10]. Also in this method, there are an inner and an outer search radius as input parameters, but the analysis is more independent from them compared to the TPI-based method. In fact, the neighborhood of the geomorphon method is self-adapting. The input radii instead have the aim to simplify the algorithm execution and bound it in the inserted areas, because otherwise, for each pixel, every time it would be achieved for all the raster. Finally, in the geomorphon method, also a flatness threshold (similar to the slope classification used in the TPI-based landform classification, but limited to areas considered flat) should be defined.

3 Study Cases

3.1 Regional Geological Framework

The comparison of the two methods of automatic extraction of landforms was carried out in three study areas belonging to different morphotectonic domains of the southern Italian chain. It is a northeast-verging fold-and-thrust belt deriving from the deformation of Mesozoic–Cenozoic shallow-water and deep-sea sedimentary succession pertained to the western border of the African-Apulian plate, and related Neogene–Pleistocene foredeep and satellite-basin deposits [15]. The foreland area is represented by the Apulian carbonate platform and represents the lower and subducting plate of the orogenic system. Starting from the Late Oligocene, the migration of the thrust front toward the north-east promoted the progressive deformation of pre-orogenic and syntectonic deposits from the inner (i.e. south-western) to the outer sectors of the belt. Pliocene-Pleistocene tectonic evolution of the chain was related to the activity of strike-slip and extensional faulting, which dismembered the contractional structure and promoted both the formation of many continental intermontane basins and the deep vertical incision of the fluvial net [16].

The landscape evolution of the southern Apennine chain was strictly related to its tectonic evolution, which in turn controlled also the distribution of the following NW-SE-trending main geological and geomorphological domains: the inner and axial zone of the chain (south-west sector), the outer zone of the chain (front of the chain/foredeep) and the foreland area (Fig. 1).

The axial zone of the chain is mainly constituted by impressive mountain ridges, bordered by steep slopes, frequently related to the activity of high-angle faults ([16] and references therein). These fault-related mountain blocks are mainly carved by erosional processes in Mesozoic shallow-water carbonate and in deep-sea sedimentary rocks of the same age. Quaternary faulting and base level lowering promoted the creation and evolution of tectonic and morphological depressions, which are crossed by longitudinal V-shaped valleys with thalwegs generally placed between 500 and 700 m of elevation a.s.l. Another peculiar feature of this sector is the presence of several orders of low-angle erosional surfaces and fluvial terraces, which are arranged in a staircase geometry between 500 and 2000 m of elevation a.s.l. ([16] and references therein).

The outer-zone and the front of the chain are featured by a NW-SE-trending thrust sheet system producing the same trend of morphostructural ridges, which are mainly carved by erosional processes affecting Cretaceous-to-Miocene pelagic deposits [15]. These units overlap the Pliocene and Pleistocene clastic deposits of the Bradano Foredeep, represented by a thick regressive succession of marine clay, and marine-to-transitional sands and gravels. The top of the foredeep succession is formed by alluvial units corresponding to large and gently-dipping plain-surfaces deeply dissected by the main rivers. These rivers exhibit a low slope gradient of longitudinal profiles in the middle/lower reaches where flow as wide braided- and meander-type fluvial patterns [17–19]. Widespread badlands also occurred in sectors where marine clay deposits crop out [20, 21].

The Foreland area is formed by an asymmetric NW–SE trending horst and graben system bordered by normal and transtensive faults inherited from late Cretaceous faulting activity. The Adriatic side (i.e.: the north-easternmost sector) of the foreland corresponds to a north-east gently-dipping carbonate landscape, which is also featured by karstic landforms and by the presence of several generations of Middle to Late Pleistocene marine terraces [22]. A well-developed drainage network cut both the karst landscape and the sequence of marine terraces: it is formed by regularly spaced and N-25–30°-trending flat-bottomed valleys with steep scarps [14].

4 Results

4.1 ACL Map of the Study Areas

High-resolution DEMs of the three test areas have been processed in order to automatically extract the main landforms of some of the geological domains of the southern Italian Apennines (Fig. 1). In order to select the most appropriate search radii in the TPI-based classification, we compared TPI values for different search radii with landforms detected through geomorphological analysis. We chose a neighborhood with an annulus shape. The dimensions of the radii chosen are reported in Table 1:

Table 1. Search radius size for the study areas (expressed in meters) in the TPI-based classification.

Areas	Smaller neighbourhood		Larger neighborhood	
	Inner radius	Outer radius	Inner radius	Outer radius
Axial zone	5	15	50	80
Foredeep area	5	15	25	40
Foreland area	8	24	40	100

Similarly, for the geomorphon-based method different input parameters where inserted and chosen after a preliminary analysis of the main landforms of the study areas carried by an "expert" geomorphological analysis. For all the three study areas it was highlighted that the best radius is of 10 cells and the flatness threshold is 1.

TPI-derived maps showed a high level of influence from the search windows and the selection of the most suitable ACL map was done through a visual inspection of "manual" landform mapping and the support of "expert" geomorphological analyses. On the contrary, ACL maps based on geomorphon highlight a low level of dependency to the input parameters and neighborhood sizes, as supposed by the study of the algorithm.

Axial Zone of the Chain

Comparison between the TPI and geomorphon classifications was carried out in a peculiar landscape of the axial zone of the chain (Fig. 1). From a geomorphological viewpoint, the test area shows a heterogeneous landscape featured by an alternation of impressive ridges with steep slopes and flat depressions.

Fluvial net is well developed and V-shaped valleys are prevalent. Moreover, a main braided river flowing into a wide floodplain (i.e. the Basento River) is placed in the north-western sector. Several orders of low-relief erosional land surfaces also occurred at the top and along the main slopes. In Fig. 2 results outcoming from the ACL analysis using the two above mentioned algorithms are shown.

The TPI-based ACL map discriminates 10 landform classes, which are distributed as follow: open slope and upper slope classes were the larger ones with a percentage of about 42% and 21%, respectively; fluvial landforms are mainly classified as U-shaped valleys (i.e. 18.7% of the total area) with a general overestimation of the “real” valleys size. Flat areas such as small intermontane basins and floodplains of main rivers are also well recognized.

The ACL map deriving from the geomorphon classification, using a line of sight of 50 m and a threshold for the flat area of 1° portrays an articulated landscape featured by a well-developed drainage network that dissects a number of ridges and slopes with different orientations. The slope class is the most representative landform whereas the flat areas exhibit a high level of noise. The map is able to delineate the fluvial net of the study area (i.e. “valley” class, Fig. 2) with a higher level of accuracy than the SPI map. Moreover, the mountain tops and ridges and the main watersheds appear well delineated.

Outer Front and Foredeep Area

The test area of this sector (Fig. 3) is a relatively «simple» landscape, since it is featured by a NE-dipping gently terraced surfaces moderately dissected by wide fluvial valleys and by the tributary fluvial net. The two ACL maps showed contrasting results (Fig. 3). In the TPI-based map, the most represented class is represented by flat areas, with a percentage of about 50.0% of the total area. Other relevant landform classes are open and upper slopes, which cover 23% and 12% of the total area, respectively. Fluvial net was largely identified as U-shaped valleys. This map shows a good potential to detect the sub-horizontal flat top terraced surface as well as the main valley flanks and their thalwegs.

The geomorphons-based map was extracted using the same search windows used for the southern Apennines axial zone and the flat threshold has been set to 1°. Slope class is the largest one with a percentage of 53% of the total area whereas the flat areas cover only 11% of the entire territory. This latter class can be associated to the undissected remnants of the terraced surfaces whereas the terrace edges are frequently classified as slope areas.

In this case, the geomorphons-based method is not able to differentiate valley flanks and gently-dipping surfaces, thus it could be useful to introduce a slope threshold, able to discriminate gently-dipping landform and steeper slopes.

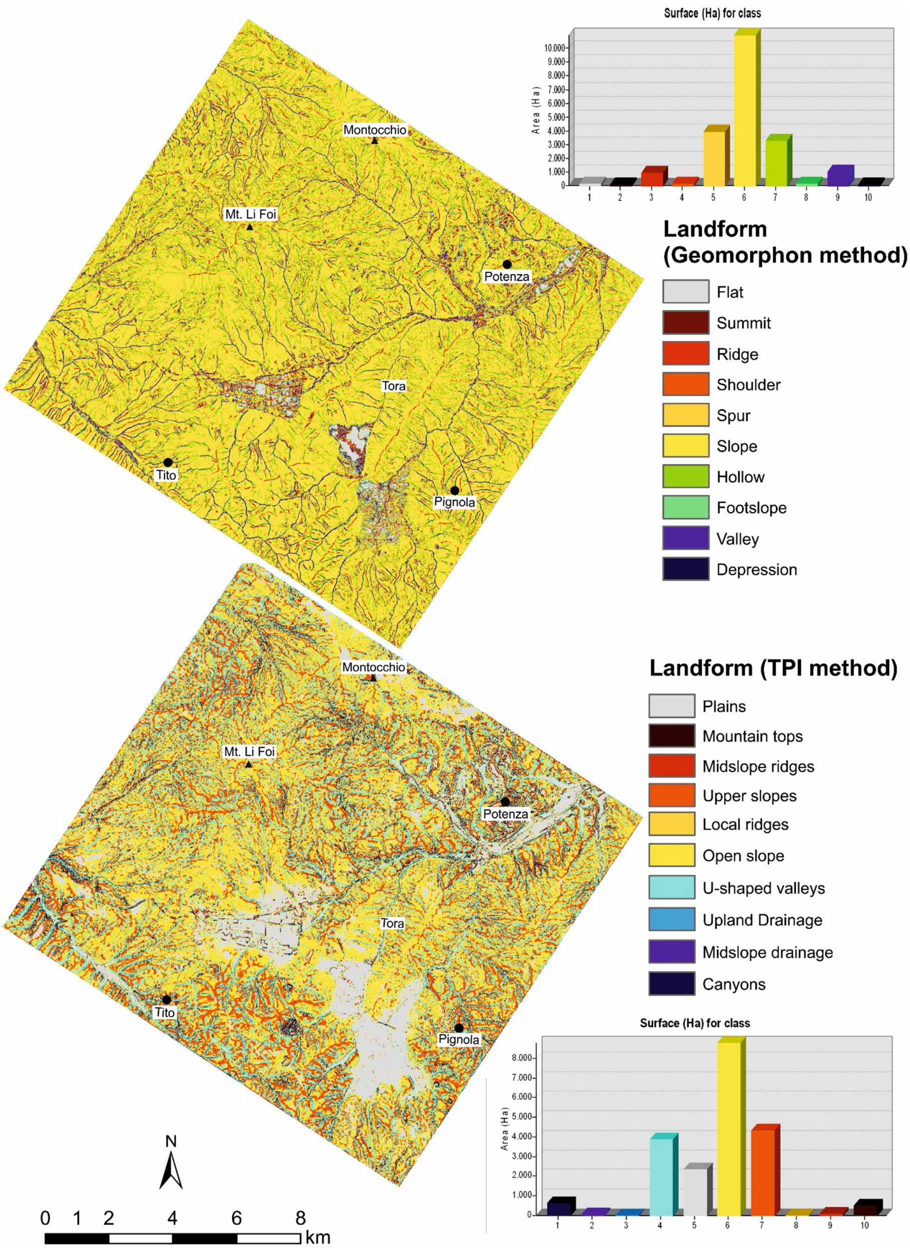

Fig. 2. ACL for axial zone of the chain

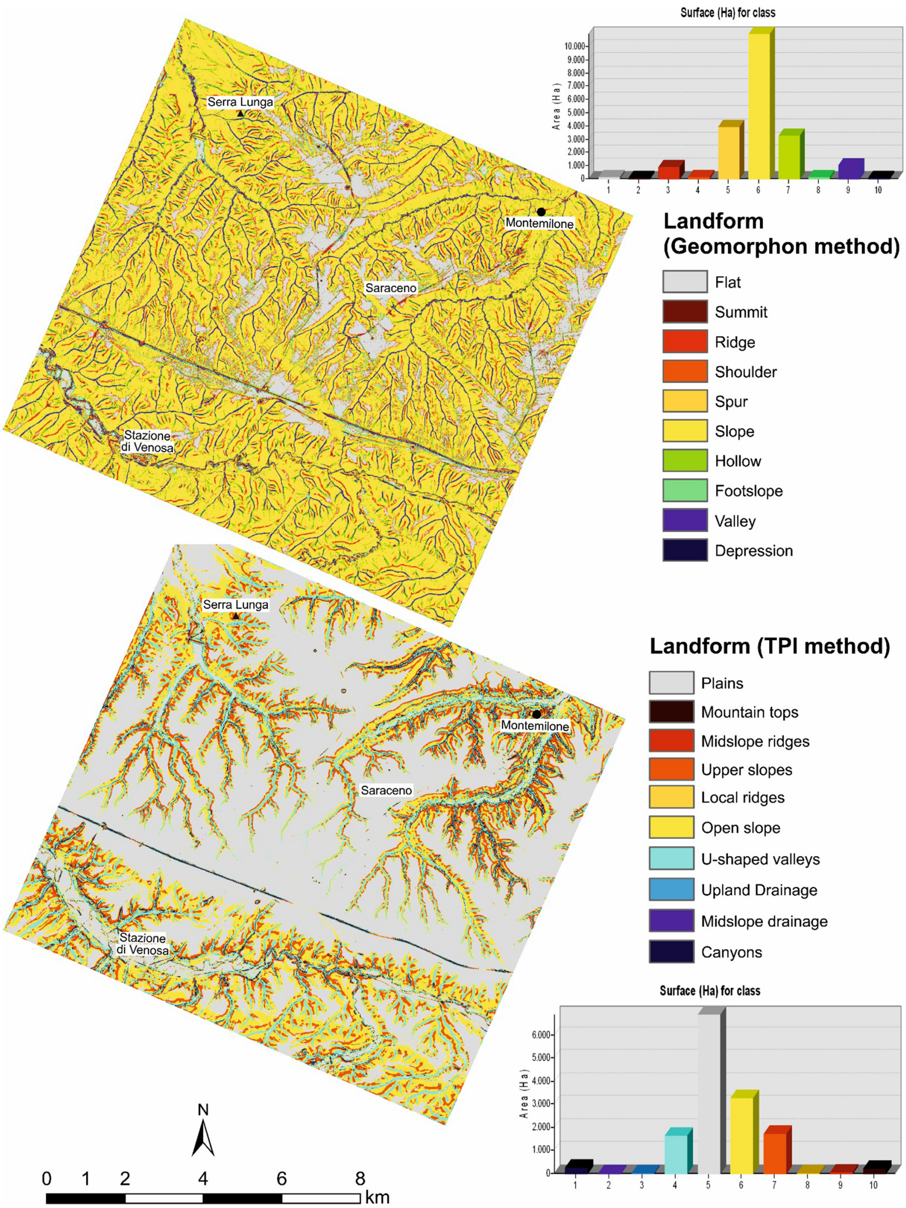

Fig. 3. ACL for the outer front and foredeep area

Foreland Area

The third study area is a small catchment of the central sector of the Apulia foreland and corresponds to a karstic landscape carved in Cretaceous shallow-water limestones (Fig. 4).

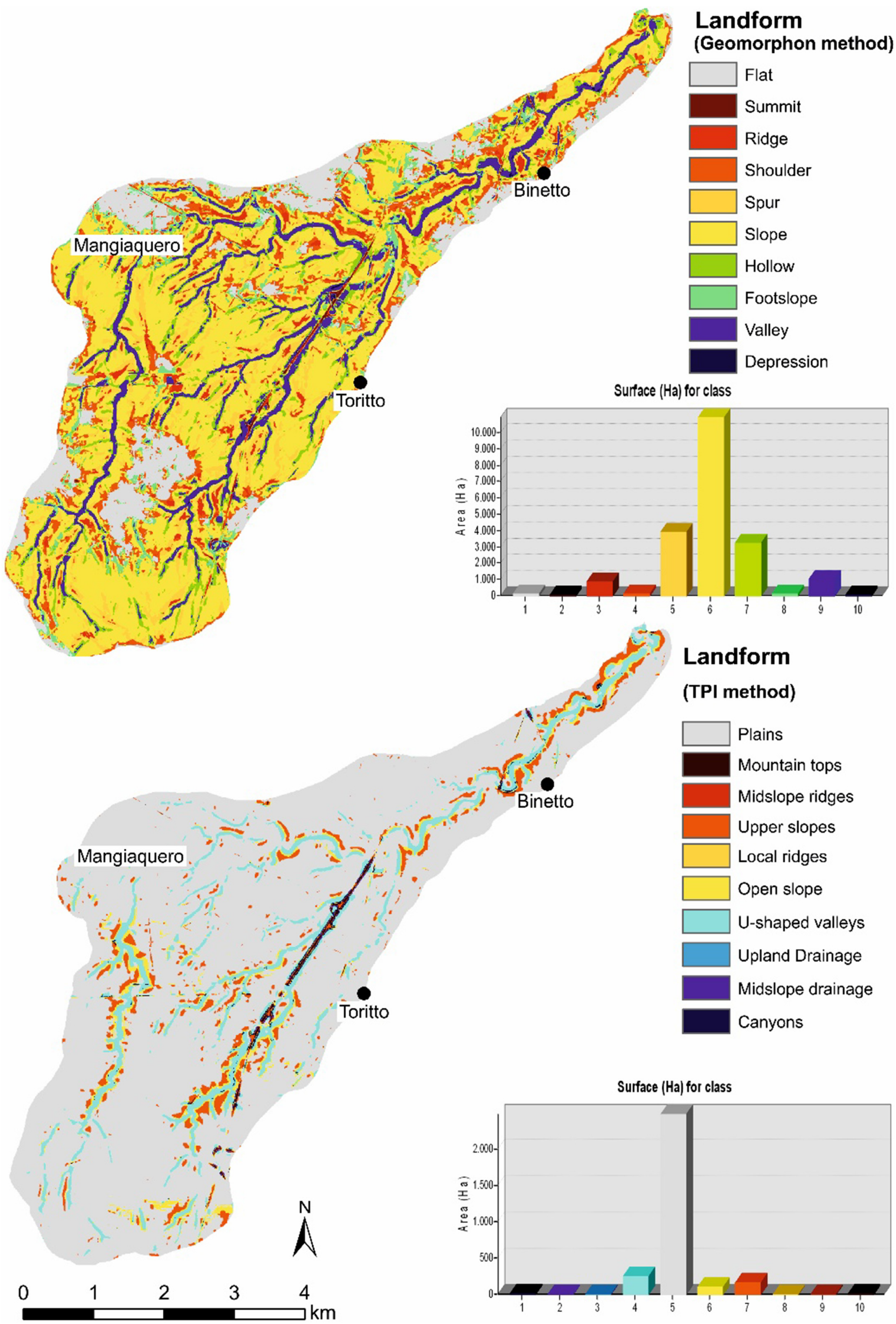

Fig. 4. ACL for the foreland area

The test area is a low-relief carbonate landscape with typical karst features and a well-defined drainage network, known as the Murge. The latter is formed by regularly spaced and N-25–30°-trending flat-bottomed valleys with steep scarps [14].

These landforms have a subtle topographic expression and are hard to recognize by classical geomorphological analyses. Recently, the application of the TPI-based landform classification at a catchment scale has been already tested as a fast and effective approach to delineate the main landforms of the Murge area [14].

TPI-based ACL map (Fig. 4) is dominated by flat areas, which represent about 80% of the total area. Flat-bottomed valleys (U-shaped valley class, see Fig. 4) and their steep flanks are discontinuously delineated.

Geomorphons-based classification was performed using the same parameters adopted for axial and foredeep areas. The map showed a better delineation of the drainage network than the TPI-based classification and related SPI map and portrayed the main fluvio-karstic landforms of the study area. Due to the general low-angle dip of the landscape, slope class is the largest one in the map but local flat areas also occurred. These sectors coincide with NW-SE-elongated sub-horizontal areas where fluvial landforms disappeared (see for example the north-westernmost sector of the map) and can be related to marine terraces related to past ancient base levels.

5 Discussion and Concluding Remarks

Advantages and limitations of two different algorithms of ACL have been investigated in three sectors of southern Italy, characterized by contrasting geological and geomorphological characters. The first element that emerges from the study is that the comparison between the two ACL methods, in order to identify the best method, is not an easy task. In fact, an extensive field control was required to verify the full suitability of the results of ACL at a large scale. Nevertheless, preliminary geomorphological analysis based on "expert" users suggested that the two algorithms could represent a basic tool to recognize the main geomorphological elements of the study areas.

Visual comparison of the ACL maps in the study areas highlights a strong difference between the two algorithms, which provided different landform classifications mainly in the foredeep and foreland sectors. Although a robust assessment of the accuracy degree of landform extraction from the two algorithms should include a detailed geomorphological mapping and a quantitative comparison from "expert" delineation of landforms and automatic classification, we provide an attempt to quantitatively compare the results coming from the two ACL methods through the grouping of landform classes of the two methods with similar features. In particular, we argued that eight of ten classes extracted by the two algorithms can be reasonably considered as similar landforms whereas two classes (i.e. footslope and hollow in the geomorphons-method; U-shaped valleys and upland drainage in the TPI classification) does not have a direct correspondence. The similarity between each class of the two methods is highlighted using the same colours in Fig. 2, 3 and 4 and allowed us to quantitatively compare the two classification methods. For example, geomorphon class "named" as plain has been interpreted as similar to the class "flat" of the TPI-method, thus we represented both with light grey.

In order to investigate the obtained results from a quantitative viewpoint, we have extracted the total number of pixels showing the similar landform in the two methods. Results highlight that differences are apparently not so high since they vary from the 7 to 17% (diagrams in Fig. 5).

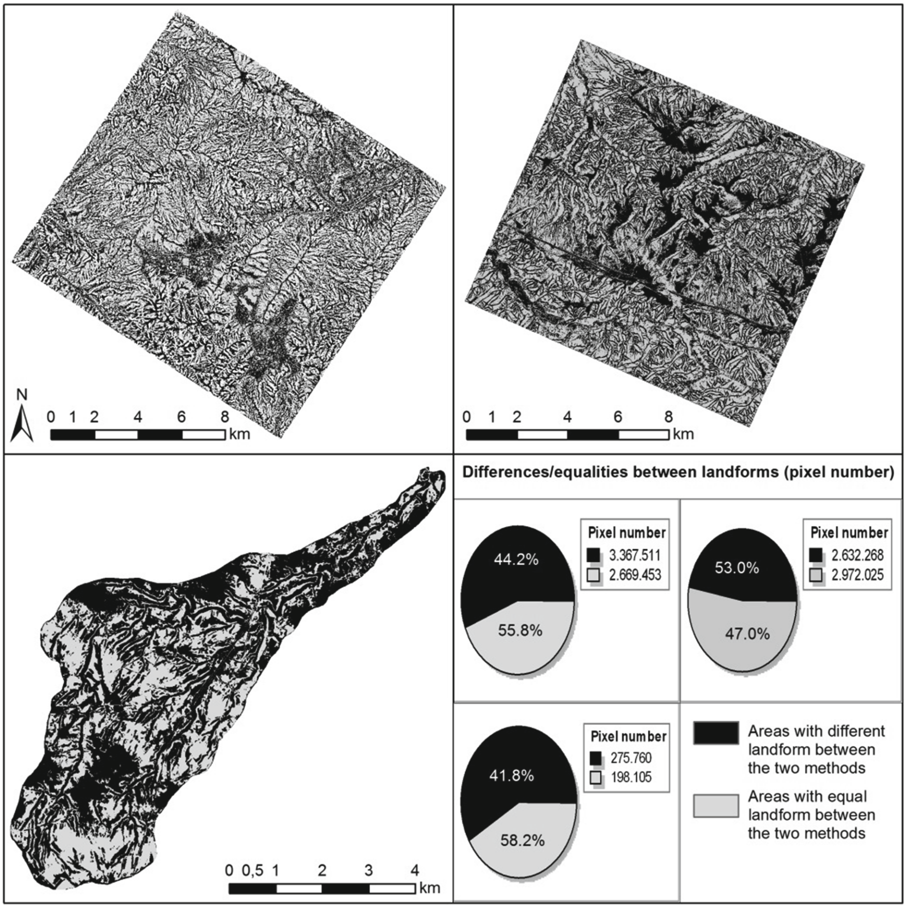

Fig. 5. Visual and quantitative comparison between the areas with similar (and different) landforms obtained from the ACL methods here used. 1) Axial zone of the chain; 2) foredeep area; 3) foreland area.

In particular, inequalities are greater than equalities in the axial zone of the chain and in the foreland area. Instead in the outer front and foredeep areas we have more similar pixel than with different landforms. However, despite to this measure, if we look at the difference/equalities maps (Fig. 5), we can see how much the results of the two methods differ and which are the hot spot of these differences: in the axial zone of the chain, geomorphons-method is able to delineate the fluvial net of the study area (i.e. “valley” class, Fig. 2) with a higher level of accuracy than the TPI map but tend to underestimate several sub-horizontal landforms of the study area such as alluvial plain and top of intermontane basins. ACL maps of the foredeep and foreland areas show more pronounced differences. In the foredeep area, the main geomorphological element (i.e. the gently-dipping terraced surfaces) is classified differently and TPI-based map is not able to detect minor fluvial channels and incisions. The geomorphons-based map portrays the undissected remnants of the terraced surfaces in a more satisfactory manner but it is not able to differentiate between the gently-dipping terrace surfaces and steeper flanks of the main valleys. A similar result can be observed in the foreland area where gemorphons-based provided a more detailed delineation of the main landforms than the TPI-based method. Also in this case, the simple introduction of a slope threshold in the geomorphons-method can help to improve the landform classification and to discriminate between peculiar geomorphological elements such as gently-dipping landsurfaces and steeper slopes related to fluvial deepening.

Our preliminary analyses suggested that geomorphons-based classification is a promising tool for automatic landform classification and can provide better results than more consolidated algorithms such as the TPI-based classification. Of course, the method needs to be deeply tested in other landscapes and/or at a wider scale but the encouraging preliminary results suggest a high potential of the proposed approach although the introduction of a slope threshold to differentiate gently-dipping and steeper slopes is required.

References

1. Hengl, T., Reuter, H.I.: Geomorphometry: Concepts, Software, Applications. Developments in Soil Science, Amsterdam (2008)
2. Wieczorek, M., Migon, P.: Automatic relief classification versus expert and field based landform classification for the medium-altitude mountain range, the Sudetes, SW Poland. Geomorphology **206**, 133–146 (2014)
3. Kramm, T., Hoffmeister, D., Curdt, C., Maleki, S., Khormali, F., Kehl, M.: Accuracy assessment of landform classification approaches on different spatial scales for the Iranian Loess Plateau. ISPRS Int. J. Geo-Inf. **6**, 366 (2017)
4. Gioia, D., Bavusi, M., Di Leo, P., Giammatteo, T., Schiattarella, M.: A geoarchaeological study of the Metaponto coastal belt, Southern Italy, based on geomorphological mapping and GIS-supported classification of landforms. Geografia Fisica e Dinamica Quaternaria **39**, 137–148 (2016)
5. Caruso, A., Clarke, K., Tiddy, C., Delean, S., Lewis, M.: Objective regolith-landform mapping in a regolith dominated terrain to inform mineral exploration. Geosciences **8**, 318 (2018)
6. De Reu, J., et al.: Application of the topographic position index to heterogeneous landscapes. Geomorphology **186**, 39–49 (2013)
7. Di Leo, P., et al.: Ancient settlement dynamics and predictive archaeological models for the Metapontum coastal area in Basilicata, Southern Italy: from geomorphological survey to spatial analysis. J. Coast. Conserv. **22**(5), 865–877 (2017). https://doi.org/10.1007/s11852-017-0548-y

8. Danese, M., Gioia, D., Biscione, M., Masini, N.: Spatial methods for archaeological flood risk: the case study of the Neolithic Sites in the Apulia Region (Southern Italy). In: Murgante, B., et al. (eds.) ICCSA 2014. LNCS, vol. 8579, pp. 423–439. Springer, Cham (2014). https://doi.org/10.1007/978-3-319-09144-0_29
9. Jenness, J., Brost, B., Beier, P.: Land facet corridor designer: extension for ArcGIS. Jenness Enterprises (2011). http://www.jennessent.com/arcgis/land_facets.htm
10. Jasiewicz, J., Stepinski, T.F.: Geomorphons—a pattern recognition approach to classification and mapping of landforms. Geomorphology **182**, 147–156 (2013)
11. Dikau, R., Brabb, E.E., Mark, R.K., Pike, R.J.: Morphometric landform analysis of New Mexico. Z. für Geomorphol. Supplementband **101**, 109–126 (1995)
12. d'Oleire-Oltmanns, S., Eisank, C., Dragut, L., Blaschke, T.: An object-based workflow to extract landforms at multiple scales from two distinct data types. IEEE Geosci. Remote Sens. Lett. **10**, 947–951 (2013)
13. Drăguţ, L., Blaschke, T.: Automated classification of landform elements using object-based image analysis. Geomorphology **81**, 330–344 (2006)
14. Teofilo, G., Gioia, D., Spalluto, L.: Integrated geomorphological and geospatial analysis for mapping fluvial landforms in Murge Basse Karst of Apulia (Southern Italy). Geosciences (Switzerland) **9**, 418 (2019)
15. Pescatore, T., Renda, P., Schiattarella, M., Tramutoli, M.: Stratigraphic and structural relationships between Meso-Cenozoic Lagonegro basin and coeval carbonate platforms in southern Apennines, Italy. Tectonophysics **315**, 269–286 (1999)
16. Schiattarella, M., Giano, S.I., Gioia, D.: Long-term geomorphological evolution of the axial zone of the Campania-Lucania Apennine, Southern Italy: a review. Geol. Carpath. **68**, 57–67 (2017)
17. Bentivenga, M., Coltorti, M., Prosser, G., Tavarnelli, E.: A new interpretation of terraces in the Taranto Gulf: the role of extensional faulting. Geomorphology **60**, 383–402 (2004)
18. Giano, S.I., Giannandrea, P.: Late Pleistocene differential uplift inferred from the analysis of fluvial terraces (southern Apennines, Italy). Geomorphology **217**, 89–105 (2014)
19. Gioia, D., Schiattarella, M., Giano, S.: Right-angle pattern of minor fluvial networks from the ionian terraced belt, Southern Italy: passive structural control or foreland bending? Geosciences **8**, 331 (2018)
20. Piccarreta, M., Capolongo, D., Bentivenga, M., Pennetta, L.: Precipitation and dry-wet cycles influence on badland development in a semi-arid area of Basilicata region (Southern Italy). Geografia Fisica e Dinamica Quaternaria **7**, 281–289 (2005)
21. Del Prete, M., Bentivenga, M., Amato, M., Basso, F., Tacconi, P.: Badland erosion processes and their interactions with vegetation: a case study from Pisticci, Basilicata, Southern Italy. Geografia Fisica e Dinamica Quaternaria **20**, 147–155 (1997)
22. Gioia, D., Sabato, L., Spalluto, L., Tropeano, M.: Fluvial landforms in relation to the geological setting in the "Murge Basse" karst of Apulia (Bari Metropolitan Area, Southern Italy). J. Maps **7**, 148–155 (2011)